LA-6378-MS

Informal Report

c. 3

UC-21

Reporting Date: September 1976

Issued: October 1976

Implosion Characteristics of Deuterium-Tritium Pellets Surrounded by High-Density Shells

by

Gary S. Fraley

los alamos
scientific laboratory
of the University of California
LOS ALAMOS, NEW MEXICO 87545

An Affirmative Action/Equal Opportunity Employer

UNITED STATES
ENERGY RESEARCH AND DEVELOPMENT ADMINISTRATION
CONTRACT W-7405-ENG. 36

Printed in the United States of America. Available from
National Technical Information Service
U.S. Department of Commerce
5285 Port Royal Road
Springfield, VA 22161
Price: Printed Copy $3.50 Microfiche $2.25

IMPLOSION CHARACTERISTICS OF DEUTERIUM-TRITIUM PELLETS

SURROUNDED BY HIGH-DENSITY SHELLS

by

Gary S. Fraley

ABSTRACT

The effect of high-density shells on deuterium-tritium pellets imploded by laser energy deposition or other means is investigated. Attention is centered on the inner parts of the pellet where hydrodynamics is the dominant mechanism. The implosions can then be characterized by a pressure boundary condition. Numerical solutions of the implosions are carried out over a wide range of parameters both for solid pellets and pellets with a central void.

I. INTRODUCTION

The implosion of small deuterium-tritium pellets driven by laser energy deposition to obtain thermonuclear fusion has been widely investigated.[1-6] It is necessary to achieve high densities (compressions of 1000 or more from solid density) to obtain efficient thermonuclear burn for pellets with masses ranging from 1 μg to 1 mg. Emphasis has been on "optimized" pulses with a typical energy deposition of the form

$$\dot{E}(t) \propto 1/(t-\tau)^2,$$

with τ a characteristic time of the pulse. Here we consider energy deposition of a less singular form but with high-density shells surrounding the thermonuclear fuel. It is expected that the high momentum density of the shells will help produce high compressions in the fuel.

The pellet consists of the fuel, the shell, and possibly other material on the outside. There may be a void in the center. Energy deposition and accompanying effects occur in the outer part of the pellet. In the interior the temperature is lower, and, if the shell is thick enough, hydrodynamics dominates the implosion. Effects in the outer part of the pellet then affect the implosion in the interior only through a pressure boundary condition, which will be applied at a constant mass point. An appropriate position for the boundary condition is at the front of the thermal or ablation wave from the outside of the pellet at the end of the implosion. It should be interior to regions significantly heated by fast electrons or radiation. Its position in the shell as a whole depends on details of effects where the laser energy is absorbed and on the shell thickness. In this report, the mass, interior to the point where the boundary condition is applied, is taken as a given quantity. Deposition of energy through the entire shell usually degrades the implosion.

The use of hydrodynamic solutions in the interior requires that the hydrodynamic energy flux, which is pressure times velocity, be much larger than that due to electron conduction or radiation. Necessary conditions on pellet size for a constant applied pressure are derived. It will be shown that typically about one-third of the implosion energy is transferred to the fuel. Then, the average applied pressure is

$$p_a = 3m_f \frac{3}{2} R\, T_i/v_f\mu_f = \frac{9}{2} \rho_f R T_i/\mu_f \; , \qquad (1)$$

where R is the gas constant, v_f is the fuel volume (the shell volume can usually be neglected), m_f, ρ_f, and μ_f are the fuel mass, density, and molecular weight, and T_i is the ignition temperature. With $T_i \approx 5$ keV $\approx 5.8\times10^7$ K. ,

$$p_a \approx 2\times10^{16}\, \rho_f \text{ ergs/cm}^3 \; , \qquad (2)$$

where ρ_f is in gm/cm^3.

We find characteristic hydrodynamic and thermal fluxes in the fuel when the initial shock has passed through the shell into the fuel. The pressure behind the shock front is $p_1 = Ap_a$, where A depends on the ratio of shell and fuel density, R_ρ. A is about 0.1 and 0.25 for $R_\rho = 100$ and 10, respectively.[7] From Eq. (1), the fuel temperature $T_f \approx p_1\mu_f/4\rho_f R \approx AT_i$. (The density behind the shock is 4 ρ_f.) The thermal conductivity $\approx 10^{19}\ \Theta^{5/2}/Z$ ergs/cm-sec-keV, where Θ is the temperature in keV and Z is the atomic number.[8] This gives a characteristic flux of $10^{21}\ A^{3.5}/r_f$ (cgs units) with r_f, the fuel radius, in cm. The jump conditions for a strong shock give a hydrodynamic flux of about $p_1^{3/2}/\rho_f^{1/2} \approx 3\times10^{24}\ A^{3/2}\ \rho_f$. If $r_f \gg 10^{-3}\ A^2/\rho_f$, the hydrodynamic flux dominates. For solid density fuel ($\rho_f = 0.2$ gm/cm^3) r_f must be much larger than a micron. Later temperatures in the fuel become increasingly uniform (except close to the center) and thermal conduction becomes less important for that reason.

In the shell, after the initial shock has passed through, the thickness is $\Delta r_s/4$ where Δr_s is the initial thickness, and from Eq. (1), the temperature $T_s \approx T_i\ \rho_f\mu_s/\mu_f\rho_s$, where ρ_s and μ_s are the shell density and molecular weight. (Typically the material is only marginally degenerate and a perfect gas equation of state may be used for calculation of the temperature.) The hydrodynamic flux $\approx p_a^{3/2}/\rho_s^{1/2} \approx 3\times10^{24}\ \rho_f^{3/2}/\rho_s^{1/2}$ (cgs units), and the thermal flux $\approx 4\times10^{21}(\rho_f\mu_s/\mu_f\rho_s)^{7/2}/Z\Delta r_s$. With $\mu_s/\mu_f \approx 3$, we require $\Delta r_s \gg 10^{-2}\ (\rho_f/\rho_s)^2/Z\rho_f$ cm.

The blackbody flux, $\sigma\, T_s^4 \approx 10^{24}\ \Theta_s^4$ ergs/cm^2-sec, where σ is the Stefan-Boltzmann constant, and Θ_s is the shell temperature in keV, is an approximate upper limit to the net radiation flux. The ratio of hydrodynamic to blackbody flux is then about $3\rho_f^{3/2}/[\rho_s^{1/2}\ (15\ \rho_f/\rho_s)^4]$ from the results previously derived. For values of $\rho_s \approx 8 - 20$ and $\rho_f \lesssim 0.2$ gm/cm^3 this is about 10 or more. If the shell is optically thick, the actual flux is approximately the blackbody flux divided by the optical depth. Radiation losses in the fuel are usually not important during the implosion. Where the applied pressure increases with time, temperatures during most of the implosion are lower and thermal conduction and radiation are correspondingly less important.

II. HYDRODYNAMIC IMPLOSIONS

A. Boundary Conditions and the Equation of State

The implosions are determined by the pressure boundary condition applied at a fixed mass point. We are interested in energy deposition with little shaping, so pressures of the type

$$p = Ct^n \qquad (3)$$

are used where n is small (0, 1, 2). A perfect gas equation of state,

$$p = \rho E(\gamma-1) \; ,$$

where E is the specific energy and $\gamma = 5/3$, is used. The initial pressure is zero. Except for the initial zero pressure, this is also the equation of state for nonrelativistic material of arbitrary degeneracy. This equation of state with one other factor, the degenerate zero temperature pressure, appears adequate for an understanding of the implosions. With this simplified model, the number of irreducible parameters (those with no scaling laws) is small enough so the calculation of a representative set of numerical solutions over the parameters becomes much more practical. With zero initial pressure, the compression achieved in the implosion depends only on the shape of the applied pressure, not its magnitude. The initial pressure acts as a cutoff, with little compression for applied pressures equal to or less than the zero temperature degenerate pressure. To illustrate details of the effect of a more realistic equation of state, calculations are also done with a Thomas-Fermi-Dirac equation of state which includes effects of degeneracy and ionization. Results are given in Sec. III.

The zero temperature degenerate pressure in the fuel is almost never important for this type of implosion, but it may be in the shell. The degenerate solution differs from the zero initial pressure case only through its effect on the initial shock that passes through the shell. The ratio of pressure before and after the shock front is positive instead of zero. The effect is small if the ratio is small. The zero temperature degenerate pressure is[9]

$$p_o = \frac{1}{5}\left(\frac{3}{8\pi}\right)^{2/3} h^2 N_o^{5/3} (\rho/\mu_e)^{5/3}/m_e$$

$$\approx 1.0\text{x}10^{13} (\rho/\mu_e)^{5/3} \text{ ergs/cm}^3 ,$$

where m_e is electron mass and μ_e is the electron molecular weight. N_o is Avogadro's constant and h is Planck's constant. The highest shell density is about 20. With $\mu_e \approx 5$ (at typical temperatures and densities behind the shock, the inner electrons are tightly bound and do not contribute to the pressure), $p_o \approx 10^{14}$. For n = 0, the pressure behind the shock is that of Eq. (1) and is $4\text{x}10^{15}$ and $1\text{x}10^{15}$ for fuel densities of 0.2 and 0.05. It is a fairly good approximation to neglect p_o for $\rho_s = 20$ and a better one for smaller ρ_s. For pellets with a void, the applied pressure is approximately $p_a/(1 + R_v)$, where R_v is the ratio of the void volume to the initial fuel volume. For $\rho_s = 20$ and $\rho_f = 0.2$, we would expect results with the realistic equation of state to fall off substantially from those with the ideal gas equation of state at $R_v \approx 40$. The initial shock with zero pressure in front achieves a compression of 4. The effect of degeneracy on applied pressures only moderately above the zero temperature pressure may approximately be taken into account by the use of the zero initial pressure solution with initial density one-fourth the density actually achieved behind the initial shock.

For n > 0, the effect is more complicated because the initial applied pressure is small. But if the applied pressure ($=p_2$) at the time the initial shock reaches the inner surface of the shell is larger (by a factor of ten or more) than the zero temperature degenerate pressure, neglect of it is a fairly good approximation. The time is roughly that required to accelerate the shell mass through one-half its thickness. The implosion time is about that required to accelerate the shell through its radius. When the work done on the pellet during the implosion time is equated to the average pressure of Eq. (1) times the displacement, we obtain the approximate result

$$p_2 \approx p_a(\Delta r_s/r_s)^{n/(n + 2)} , \qquad (4)$$

with r_s being the initial shell radius.

B. Scaling Laws

The perfect gas solutions scale for all but three or four parameters: R_ρ, the ratio of shell over fuel density; R_m, the ratio of shell mass (inside the boundary condition point) over fuel mass, n, and for pellets with a central void; R_v, the ratio of volume of the void to initial fuel volume. The scaling laws show that maximum densities are independent of C [in Eq. (3)], while temperatures do depend on it, so there is density-temperature decoupling.

The scaling laws are found as follows: let $p_1(m,t)$, $r_1(m,t)$, $v_1(m,t)$, and $u_1(m,t)$ be the pressure, radius, specific volume, and velocity of the solution for a system with unit mass and unit specific volume in the fuel. The Lagrangian variable m is the mass interior to a point, and t is the time. The applied pressure is

$$p_1(1,t) = t^n .$$

The initial pressure is $p_1(m,0) = 0$. Consider solutions of the type

$$\begin{aligned} p(m,t) &= C_2\, p_1(m/m_t,\ C_1 t) ,\\ r(m,t) &= C_4\, r_1(m/m_t,\ C_1 t) ,\\ v(m,t) &= C_3\, v_1(m/m_t,\ C_1 t) , \end{aligned} \qquad (5)$$

and

$$u(m,t) = C_1 C_4 u_1(m/m_t,\ C_1 t) ,$$

where m_t is the total mass. The equation of state is

$$E = pv/(\gamma-1) \quad ,$$

where $\gamma = \gamma(m/m_t)$ only. The applied pressure is

$$p(m_t, t) = C_1^n C_2 t^n = Ct^n \quad . \qquad (6)$$

From the equations of motion,

$$\frac{\partial u}{\partial t} = 4\pi r^2 \frac{\partial p}{\partial m} \quad ,$$

$$\frac{\partial E}{\partial t} + p \frac{\partial v}{\partial t} = 0 \quad , \qquad (7)$$

$$u = \frac{\partial r}{\partial t} \quad ,$$

and

$$v = 4\pi r^2 \frac{\partial r}{\partial m} \quad ,$$

we have

$$C_1 = C^{\frac{1}{n+2}} m_t^{-\frac{2}{3(n+2)}} \rho_f^{-\frac{1}{3(n+2)}} \quad ,$$

$$C_2 = C\, C_1^{-n} \quad , \qquad (8)$$

$$C_3 = \rho_f^{-1} \quad ,$$

and

$$C_4 = m_t^{1/3} \rho_f^{-1/3} \quad .$$

III. RESULTS

A. Implosions with No Central Void

The solutions were calculated with a standard-type spherically symmetric Lagrangian code with explicit hydrodynamics. Shock waves are handled by artifical viscosity. Values of R_ρ of 40, 100, and 400 were used, corresponding to ρ_f = 0.2 and ρ_s = 8 and 20, and ρ_f = 0.05 and ρ_s = 20. For these values mass ratios from 10 to 100 are most interesting. Maximum fuel compression is achieved in this range. The transfer efficiency, the ratio of energy transferred to the fuel over the total implosion energy, is large enough at R_m = 10 so that it cannot increase much for smaller mass ratios. There are three important output parameters: the transfer efficiency, the maximum fuel ρ-R, and total ρ-R with ρ-R ≡ $\int \rho dr$. The last two are conveniently normalized by the initial fuel ρ-R.

In a pellet consisting only of compressed fuel, the effective reaction time is the time it takes a rarefaction wave from the surface to reach a mass element.[4] This disassembly time, averaged over the fuel, is $r_F/(4C_f)$ where C_f is the sound speed. The reactions per mass, N_m, are proportional to the product of the reaction rate, $\langle\sigma V\rangle \rho_f$, with the reaction time, where $\langle\sigma V\rangle$, the product of the averaged fusion cross section and velocity, depends only on temperature.

$$N_m \propto \langle\sigma V\rangle \rho_f r_f/(4C_f).$$

This can be factored into the $\rho\text{-}R_f$ and a function of temperature.

With a high-density shell, the implosion ends with the fuel and the inner highly compressed part of the shell all at about the same pressure. The reaction time is increased by the time it takes a rarefaction to cross the compressed part of the shell. The solutions show that, if at the end of the implosion the shell thickness is not more than about the fuel radius (which includes most cases calculated here), most of the shell ρ-R comes from the inner compressed part. Then,

$$N_m \propto \langle\sigma V\rangle \rho_f (r_f/4\, C_f + \Delta r_s'/C_s) \qquad (9)$$

with $\Delta r_s'$ being the width of the compressed part of the shell and C_s being the speed of sound. With

$$C_s \approx C_f (\rho_f/\rho_s)^{1/2} ,$$

$$N_m \propto \frac{\langle\sigma V\rangle}{C_f} [\rho\text{-}R_f/4 + \rho\text{-}R_s(\rho_f/\rho_s)^{1/2}] \quad . \qquad (10)$$

Usually, to within a factor of two, the density ratio is established when the first strong shock hits the fuel-shell interface. For[7] $R_\rho \gg 1$,

$$(\rho_f/\rho_s)^{1/2} \approx 0.5/R_\rho^{0.2}$$

$$\approx 1/5 \text{ for } R_\rho = 100 \quad . \qquad (11)$$

It is not a strong function of R_ρ. The shell ρ-R

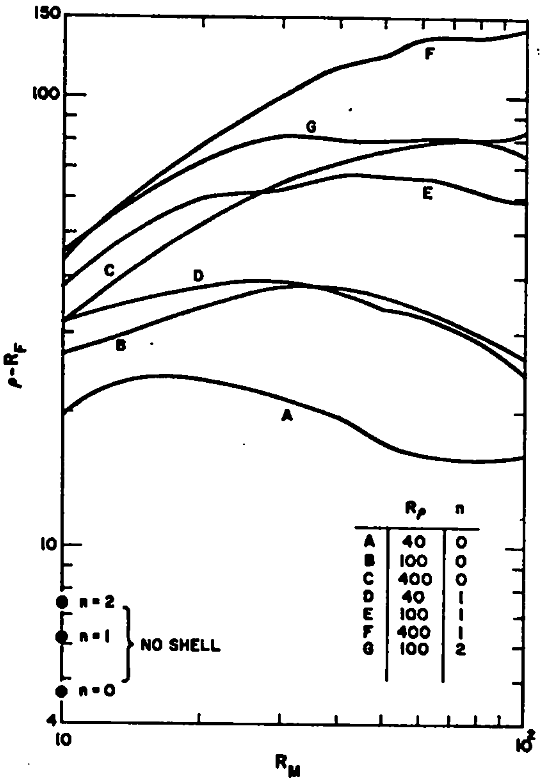

Fig. 1. Fuel ρ-R for pellets with no central void.

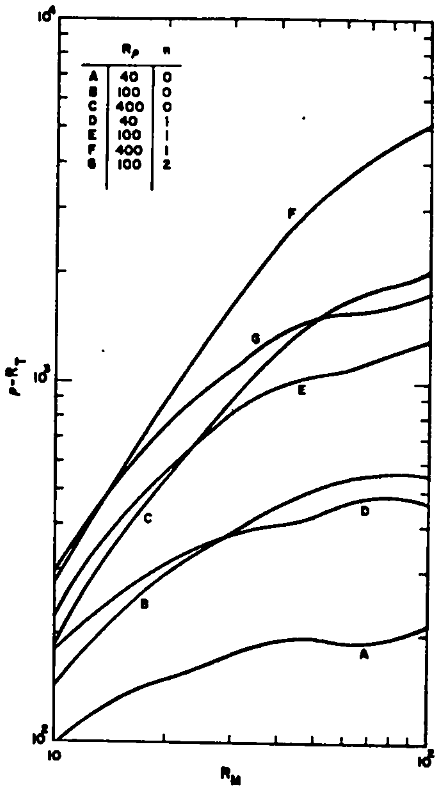

Fig. 2. Total ρ-R.

is typically as effective as the fuel ρ-R; the figure of merit is the total ρ-R. The ρ-R_f is still important for effects as alpha particle deposition.

Figure 1 gives the normalized ρ-R_f. It increases as n and R_ρ increase, and varies from about 20 to 150. The ρ-R for bare pellets varies from 5 to 7 for n = 0, 1, 2. The mass ratio varies from about 15 to 100 for maximum ρ-R_f for different R_ρ. This roughly corresponds to an aspect ratio $(r_s/\Delta r_s)$ of ten. Figure 2 gives the total ρ-R for the same cases; this varies from 10^2 to almost 10^4. Figure 3 gives energy transfer efficiency. It is typically about one-third for those mass ratios which give maximum ρ-R_f. The transfer efficiency also increases with R_ρ and n.

At the beginning of the implosion, the boundary pressure forms a shock in the shell. When it reaches the fuel, the shock continues through the fuel and a rarefaction propagates back through the shell. The shock is reflected at the center and is again reflected at the fuel-shell interface. Further shocks are usually weak and may be ignored. The fuel

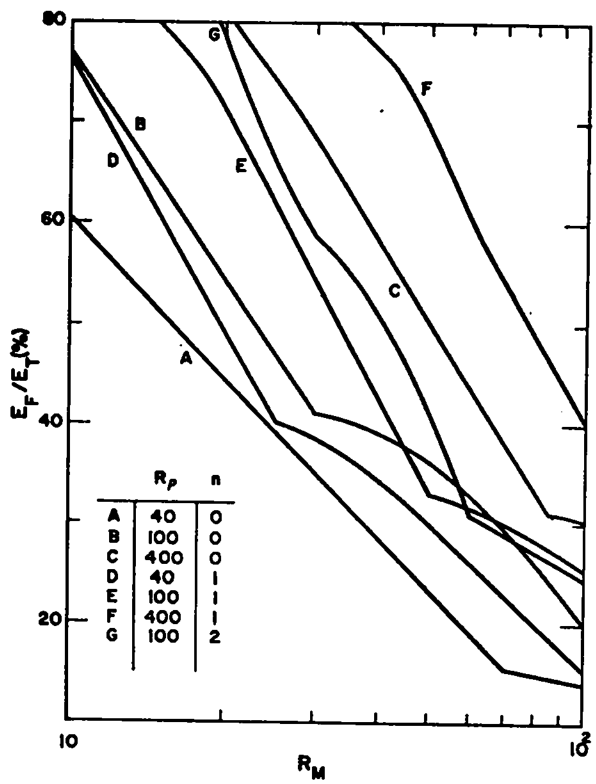

Fig. 3. Transfer efficiency.

is then nearly isentropically compressed as it continues to decelerate the shell. The compression increases with shell mass (and momentum) until, for sufficiently large R_m, the outer part of the shell remains too far away from the fuel to contribute to its compression. A pressure pulse originates at the outer boundary when it is reached by the rarefaction. The pulse propagates through the shell and fuel, and tends to turn the reflected shock from the center around in the fuel before it reaches the shell. This allows for more isentropic compression. The timing of the pulse is most effective at about the value of R_m which produces the maximum fuel ρ-R. For larger R_m the $\rho\text{-}R_f$ decreases to an asymptotic value.

The shock formed in the fuel (and its reflection) is weaker compared with the original shock in the shell for larger R_ρ. This allows more of the nearly isentropic compression after the transit of the first strong shocks. The total compression is then greater for larger R_ρ. Higher values of n produce a weaker initial shock and allow compression on a lower adiabat.

Figures 4 and 5 give results using the Thomas-Fermi-Dirac equation of state. The fuel and shell density and type of material, and the constant in Eq. (3) must be specified, besides the parameters n, R_ρ, and R_m required for the perfect gas equation of state. Deuterium-tritium fuel densities of 0.05 and 0.2 were used. For shell densities of 8 and 20, iron and gold were used. The perfect gas solutions, plus the scaling rules, give the value of C which will produce a given average temperature in the fuel at maximum compression. The value of C giving an average temperature of 4 keV was chosen. The actual temperature with the Thomas-Fermi-Dirac equation of state was usually within 10% of 4 keV. Because of the low sensitivity of the output parameters on C, there were no further adjustments in its value. By Eq. (4), we expect the results for R_ρ = 400, n = 1 to begin to fall off from the perfect gas solutions. This is observed, the worst case giving about 55% the perfect gas ρ-R. For other R_ρ and n, the compression was occasionally somewhat greater than that of the perfect gas solution. This seemed to be caused by a higher shell density behind the initial shock, due to ionization effects on the equation of state. The compression was as large as 5,

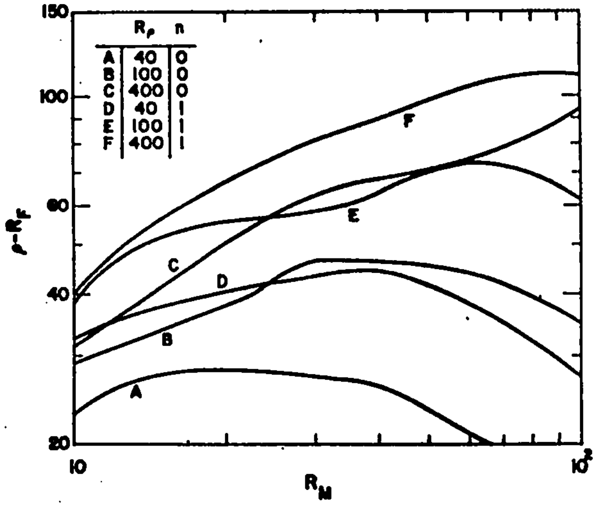

Fig. 4. Fuel ρ-R for Thomas-Fermi-Dirac equation of state.

instead of the factor of 4 for a perfect gas with γ = 5/3.

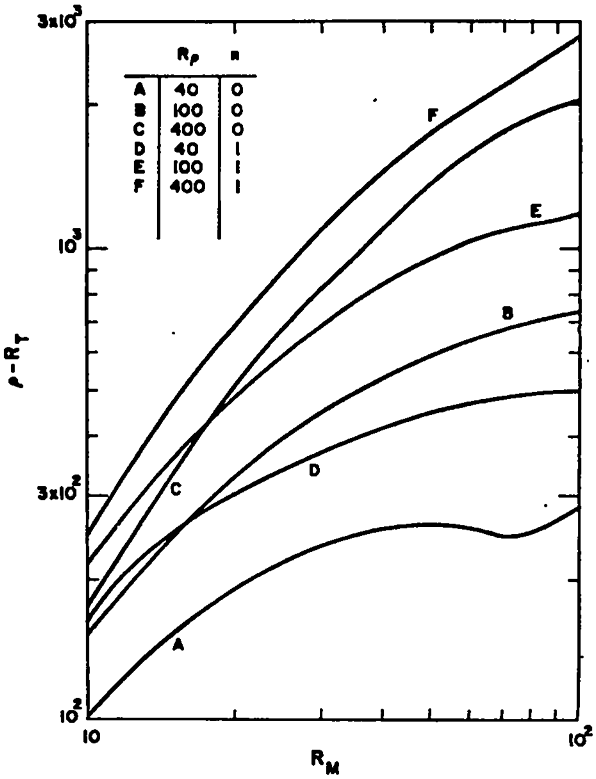

Fig. 5. Total ρ-R for Thomas-Fermi-Dirac equation of state.

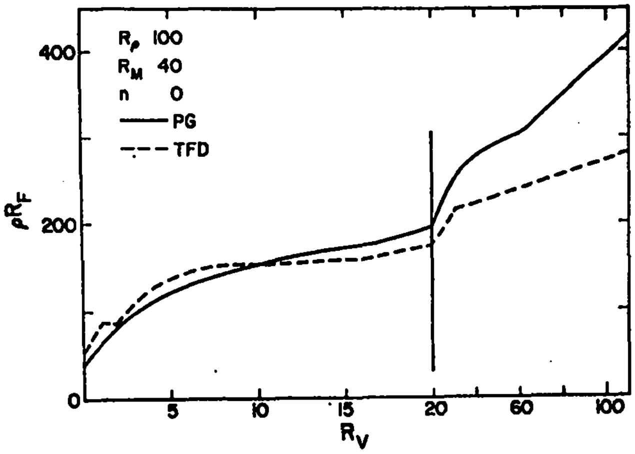

Fig. 6. Fuel ρ-R for pellets with central void for Thomas-Fermi-Dirac and perfect gas equations of state.

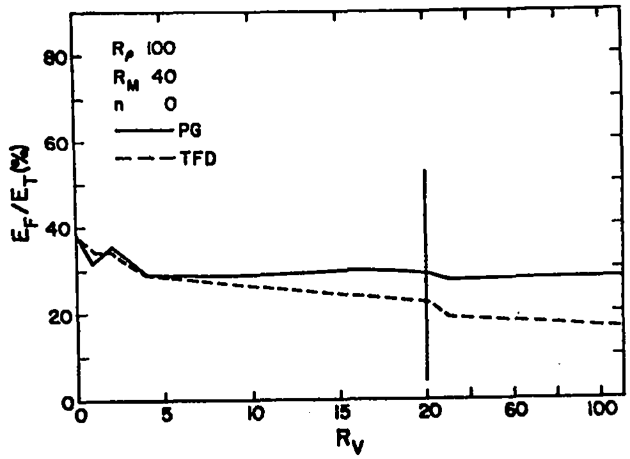

Fig. 8. Transfer efficiency.

B. Implosions With a Central Void

Figures 6, 7, and 8 give results for pellets with a void in the center. (The ρ-R is normalized in terms of the initial fuel ρ-R for the fuel in a solid sphere at the center.) The constant in the boundary pressure for the Thomas-Fermi-Dirac equation of state was chosen in the same way as before. For large R_v, after the initial shocks and rarefactions, the internal energy of the material remains nearly constant until it approaches the center. The applied pressure goes into kinetic energy. When the material hits the center, a shock propagates outward. Most of the compression comes from isentropic spherical convergence before and after passage of the shock. For this reason compression is more than that due to just one strong shock. For a perfect gas equation of state, it appears that compression increases indefinitely as R_v increases. (The large values of R_v are probably not realistic as we would not expect these cases to retain sufficient spherical symmetry.) For the Thomas-Fermi-Dirac equation of state, the applied pressure necessary for ignition decreases as R_v increases, and it becomes comparable to the degenerate pressure in the shell. This causes the results to fall off compared with the perfect gas cases.

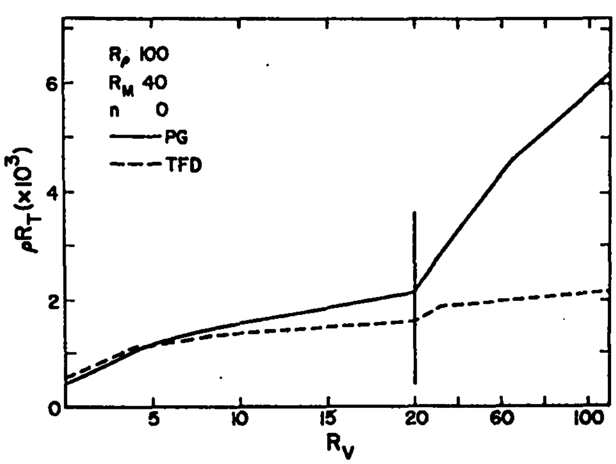

Fig. 7. Total ρ-R.

IV. CONCLUSION

The (normalized) ρ-R for no shell was about 5 for n = 0 and 7 for n = 2. For the case (R_ρ = 100, R_m = 40, n = 0), the total ρ-R is about 600. The use of shells for energy input pulses with little shaping can increase the ρ-R by 100 or more. From Sec. III this increases the yield by the same factor. Since the typical transfer efficiency is about a third, the fuel mass (for a given implosion energy and the same fuel temperature) is decreased by a factor of three. The net yield is then increased by about 25.

The linear relationship between yield and ρ-R neglects the heating due to thermonuclear burn. This in effect produces a nonlinear dependence of yield on ρ-R. The most interesting case is in the strong nonlinear region. For a 0.1-mg pellet with density 0.2, the initial ρ-R is 0.01. A constant boundary pressure gives a final ρ-R of 0.05. For a temperature at end of implosion of 3 keV, this has a burn efficiency of 5×10^{-5} (Ref. 4). Surrounding that with a gold shell of 4 mg gives a final ρ-R of about 6 and a burn efficiency of 0.6.

The crucial factor in obtaining efficient thermonuclear burn in this type of pellet is to achieve a fuel ρR which is sufficient to stop alpha particles.[4] This is about 0.5 gm/cm^2. If this is achieved, the reaction time, which depends on the total ρR, will usually be large enough for efficient burn. For solid density deuterium-tritium, an increase in the ρR_f of a factor of about 60 may be obtained for pellets with no central void (Fig. 4, Line E). The fuel mass required is roughly 0.05 mg, which has a reaction energy of 16 megajoules, the equivalent of about 2. kg(5lb) of high explosive. With a transfer efficiency of one-third, 75 kilojoules are needed for the implosion. The total energy required depends on the efficiency with which it is applied to the implosion; for an efficiency of 10%, somewhat less than 1 megajoule is required. Much higher compressions are possible with the use of voids, and this lowers the mass and energy requirements. The limiting factor will be the spherical symmetry that can be achieved. For pellets of marginal size, the best mass ratio (R_m) is that which gives the maximum ρR_f. This is typically given by an aspect ratio of the shell of about 10. Because the transfer efficiency usually increases rapidly with a decreasing mass ratio at this point, the best ratio for larger pellets will be several times smaller where the transfer efficiency is close to one.

REFERENCES

1. J. Nuckolls, T. Wood, A. Thiessen, and G. Zimmerman, Nature (Lond) 239, 139 (1972).

2. J. S. Clarke, H. N. Fisher, and R. J. Mason, Phys. Rev. Lett. 30, 89 (1973); Phys. Rev. Lett. 30, 249 (1973).

3. K. Brueckner, IEEE Trans. Plasma Sci. PS-1, 13 (1973); K. Brueckner and S. Jorna, Rev. Mod. Phys. 46, 325 (1974).

4. G. S. Fraley, E. J. Linnebur, R. J. Mason, and R. L. Morse, Phys. Fluids 17, 474 (1974).

5. R. Kidder, Nucl. Fusion 14, 53 (1974).

6. R. J. Mason and R. L. Morse, Phys. Fluids 18, 816 (1975).

7. F. Harlow and A. Amsden, Los Alamos Scientific Laboratory Report No. LA-4100, (1970).

8. L. Spitzer, Physics of Fully Ionized Gases, Interscience, New York, (1962).

9. J. Cox and R. Giuli, Principles of Stellar Structure, Gordon and Breach, New York, (1968).